UCLA

Title

PARP12 suppresses Zika virus infection through PARP-dependent degradation of NS1 and NS3 viral proteins

Permalink

https://escholarship.org/uc/item/31q2z8s1

Journal

Science Signaling, 11(535)

ISSN

1945-0877

Authors

Li, Lili
Zhao, Hui
Liu, Ping
et al.

Publication Date

2018-06-19

DOI

10.1126/scisignal.aas9332

Peer reviewed

PARP12 suppresses Zika virus infection through PARP-dependent degradation of NS1 and NS3 viral proteins

Lili Li[1,2], **Hui Zhao**[3], **Ping Liu**[1], **Chunfeng Li**[4,5], **Natalie Quanquin**[6], **Xue Ji**[3], **Nina Sun**[1,2], **Peishuang Du**[1], **Cheng-Feng Qin**[3], **Ning Lu**[1,*], and **Genhong Cheng**[4,5,6,*]

[1]CAS Key Laboratory of Infection and Immunity, Institute of Biophysics, Chinese Academy of Sciences, Chaoyang District, Beijing 100101, China.

[2]University of Chinese Academy of Sciences, Beijing 100101, China.

[3]Department of Virology, State Key Laboratory of Pathogen and Biosecurity, Beijing Institute of Microbiology and Epidemiology, Beijing 10071, China.

[4]Center for System Medicine, Institute of Basic Medical Sciences, Chinese Academy of Medical Sciences and Peking Union Medical College, Beijing 100005, China.

[5]Suzhou Institute of System Medicine, Suzhou, Jiangsu 215123, China.

[6]Department of Microbiology, Immunology and Molecular Genetics, University of California, Los Angeles, CA 90095, USA.

Abstract

Zika virus infection stimulates a type I interferon (IFN) response in host cells, which suppresses viral replication. Type I IFNs exert antiviral effects by inducing the expression of hundreds of IFN-stimulated genes (ISGs). To screen for antiviral ISGs that restricted Zika virus replication, we individually knocked out 21 ISGs in A549 lung cancer cells and identified PARP12 as a strong inhibitor of Zika virus replication. Our findings suggest that PARP12 mediated the ADP-ribosylation of NS1 and NS3, nonstructural viral proteins that are involved in viral replication and modulating host defense responses. This modification of NS1 and NS3 triggered their proteasome-mediated degradation. These data increase our understanding of the antiviral activity of PARP12 and suggest a molecular basis for the potential development of therapeutics against Zika virus.

INTRODUCTION

A mosquito-borne flavivirus similar to dengue virus (DENV) and West Nile virus (WNV), Zika virus (ZIKV) has drawn global attention due to its rapid spread across the Pacific to the Americas (1, 2) and growing reports of fetal microcephaly and other congenital abnormalities (3, 4). Although infection is most often asymptomatic (5–7), the causal relationship between ZIKV infection during pregnancy and fetal microcephaly is now proven (6, 8–10). There are currently no effective treatments or vaccines. Therefore, a better understanding of ZIKV pathogenesis and host-virus interactions is urgently needed.

ZIKV has a single-stranded positive RNA genome that is translated into a large polyprotein. That protein is then proteolytically processed by host and viral proteases to produce three structural proteins referred to as the capsid protein (C), premembrane/membrane protein (prM/M), and envelope glycoprotein (E), as well as seven nonstructural proteins (NS1, NS2A, NS2B, NS3, NS4A, NS4B, and NS5) (11). C, E, and prM/M proteins and the enveloped viral genome constitute the mature viral particle. The nonstructural proteins are involved in replication and assembly of the virus and in antagonizing the host innate immune response and have been a focus of intensive research. For example, NS1 modulates the host antibody response and may contribute to viral immune evasion strategies (12, 13). NS2B, NS4A, and NS4B are believed to inhibit the production of type I interferon (IFN) by host immune cells (14, 15). In addition, NS3, which has protease activity, in combination with NS2B may cleave and inactivate the mitochondrial-bound sensor of cytosolic nucleic acid stimulator of interferon genes (16). Further description of ZIKV nonstructural protein function is fundamental for understanding host-ZIKV interactions.

As key components of the innate immune system, IFN and hundreds of IFN-stimulated genes (ISGs) provide a critical defense against viral pathogens (17, 18). These ISGs work as antiviral effectors, many of which are poorly described. There is evidence indicating that ZIKV infection triggers type I IFN production by host cells, and ZIKV is sensitive to the antiviral activity of IFN (19, 20). For example, cholesterol-25-hydroxylase and its enzymatic product, 25-hydroxycholesterol, are critical mediators of host protection against ZIKV infection and its associated microcephaly in a mouse model (20). Herein, we identify *PARP12*, an ISG whose expression was induced by IFN-α/β, as an inhibitor of ZIKV replication. PARP12 belongs to the family of poly–adenosine 5′-diphosphate (ADP)–ribose polymerases (PARPs), also known as ADP-ribosyltransferases (21), which catalyze the transfer of ADP-ribose from nicotinamide adenine dinucleotide (NAD^+) to targeted proteins in a unique translational modification called ADP-ribosylation (22). Humans express 17 PARPs, which play roles in diverse cellular responses, such as stress including DNA damage repair, the heat shock response, the unfolded protein response, the cytoplasmic stress response, and the antiviral response (23–25). Several studies indicate that the involvement of PARPs in the mammalian antiviral response is widespread, with the regulation of both viral and antiviral defense transcripts (26–29).

There are two splice forms of the *PARP12* mRNA and translation into two PARP12 isoforms, the large one (PARP12L) and the short one (PARP12S) that lacks the C-terminal PARP domain (30). *PARP12L* is an antiviral ISG involved in regulating protein translation

and inflammation (30–33). Although an antiviral function for PARP12 has been reported (31, 33), the exact mechanism has never been described. Here, we identified the long isoform *PARP12* as an antiviral ISG that effectively restricted ZIKV replication in vitro. Furthermore, our work showed that PARP12 suppressed ZIKV by promoting the degradation of NS1 and NS3 proteins through the ubiquitin-proteasome pathway in a manner that required PARP domain–mediated enzyme activity.

RESULTS

The ISG *PARP12* suppresses ZIKV replication in vitro

To identify ISGs with activity against ZIKV, we screened 21 clustered regularly interspaced short palindromic repeats (CRISPR)/CRISPR-associated protein 9 (Cas9) knockout A549 cell lines for sensitivity to ZIKV infection (table S1). We chose ISGs for our screen with (*CH25H, PARP12, PARP11, PVRL4, OASL, IRF1, TRIM5, CASP2, TRIM21, SERPINA4, IFIT1*, and *GPR146*) and without (*ALDH1B1, ACSL3, ACSL5, AKT1, ETNK1, TYMP, MLKL, PIK3IP1*, and *GDF10*) known antiviral activity (17, 33). These verified knockout cells were then infected with ZIKV, and virus in the culture supernatants was quantified by plaque assay (fig. S1A). Cells lacking *PARP12* supported greater ZIKV replication at 24 hours after infection than other ISG-knockout cells (Fig. 1A), and a ZIKV production was about five times more than wild-type (WT) control at 48 hours after infection (fig. S1B). Given these results, we chose to further examine the role of PARP12 in restricting ZIKV replication.

To characterize the induction of PARP12 by IFN, we stimulated WT and IFN-α receptor (IFNAR1)–deficient A549 cells with human IFN-α, IFN-β, or IFN-γ and quantified the number of *PARP12* mRNA transcripts by quantitative real-time polymerase chain reaction (qRT-PCR). IFNAR1 is a receptor for type I IFNs, and its absence should impair IFN-α and IFN-β signaling but not affect the function of IFN-γ (a type II IFN). We found that increased *PARP12* mRNA was induced by all three types of IFN in WT A549 cells but most strongly by IFN-α (fig. S2A). This effect required IFNAR1 expression in A549 cells (fig. S2A). Similar to exogenous IFN treatment, ZIKV infection also increased *PAPR12* mRNA expression in WT A549 cells but not in *IFNAR1*$^{-/-}$ A549 cells (fig. S2B). To further characterize the function of PARP12, we generated both PARP12-knockout (fig. S3, A to C) and stable PARP12-overexpressing A549 cells (fig. S3D). We found that ZIKV replication was suppressed in cells overexpressing PARP12 (Fig. 1, B to D). Conversely, ZIKV replicated more robustly in *PARP12*$^{-/-}$ A549 cells (Fig. 1, E to G). Similar results were found when we measured ZIKV replication in primary mouse embryonic fibroblast (MEF) that either lacked or overexpressed PARP12 (Fig. 1, H and I). These results demonstrate that *PARP12* is an antiviral ISG induced by both IFN and ZIKV infection, which inhibits ZIKV replication.

PARP12 suppresses ZIKV by decreasing the abundance of NS1 and NS3 proteins

To elucidate the mechanism by which PARP12 suppressed ZIKV infection, we sequentially examined steps of the viral life cycle by assessing viral binding, entry, and replication (20, 34). Binding and entry assays showed that PARP12 had no effect on the early step of ZIKV

infection (Fig. 2, A and B). We next used a subgenomic replicon system that encodes the seven ZIKV nonstructural proteins with a *Renilla* luciferase (*RLuc*) reporter to measure viral replication activity. Over expression of PARP12 reduced the replication of the ZIKV RNA genome (Fig. 2C).

Reduced ZIKV replication activity may result from decreased protein abundance of one or more nonstructural proteins important for viral replication. To test this, we cotransfected human embryonic kidney (HEK) 293T cells with plasmids encoding PARP12 and one of the seven ZIKV nonstructural proteins (NS1, NS2A, NS2B, NS3, NS4A, NS4B, or NS5). PARP12 coexpression reduced the abundance of ZIKV NS1 and NS3 proteins but not of other ZIKV nonstructural proteins (Fig. 2, D and E). We did not detect NS2A protein in our studies. When we cotransfected HEK293T cells with either NS1, NS3, or NS4A plasmids and increasing amounts of PARP12 expression plasmid, we found that NS1 and NS3 abundance decreased gradually with increasing amounts of PARP12, but the abundance of NS4A showed no obvious change (Fig. 2, F and G). Furthermore, when endogenous *PARP12* was knocked out, more NS1 and NS3 proteins accumulated after transfection of *PARP12*$^{-/-}$ cells than WT control cells. Reconstitution of *PARP12*$^{-/-}$ HEK293T cells with PARP12 reduced the abundance of NS1 and NS3 proteins (Fig. 2, H and I). Similarly, the production of NS1 and NS3 proteins in WT and *PARP12*$^{-/-}$ A549 cells infected with ZIKV was increased in *PARP12*$^{-/-}$ cells compared to WT control cells (Fig. 2, J and K). Together, these results suggest that PARP12 suppresses ZIKV replication by specifically reducing the abundance of NS1 and NS3 proteins.

The PARP domain of PARP12 is required for control of ZIKV NS1 and NS3 protein abundance

In addition to the PARP domain, PARP12 has four CCCH-type Zinc-finger (ZnF) domains at the N terminus and one WWE domain at its center (Fig. 3A). The ZnF domains of related proteins are involved in viral mRNA silencing and transcription suppression (26, 35). The ZnF domains of PARP13 can bind to viral RNAs and target them for degradation by recruiting cellular mRNA decay factors and interfering with the interaction between translational initiation factors eIF4G and eIF4A to suppress translation (26, 36, 37). The WWE domain is a common interaction module in both protein ubiquitylation and ADP-ribosylation (38). The PARP domain mediates the posttranslational modification of target proteins, such as poly-ADP-ribosylation (PAR) and ubiquitylation (39, 40).

To identify which domain of PARP12 was responsible for controlling ZIKV infection, we generated domain deletion mutants (Fig. 3A). The expression and expected size of the mutations were verified by Western blotting (fig. S4). The mutations were cotransfected with His-NS1 or NS3 into *PARP12*$^{-/-}$ HEK293T cells, and the abundance of NS1 and NS3 proteins was measured by immuno-blotting (Fig. 3, B and C). We found that PARP12 overexpression had no impact on *NS1* and *NS3* mRNA expression (Fig. 3D), suggesting that the effect of PARP12 was not mediated at the mRNA level. Similarly, deletion of the ZnF domains that bind mRNA in PARP12 did not impair the loss of NS1 or NS3 protein (Fig. 3, B and C), despite the homology between the ZnF domains of PARP12 and PARP13 (fig. S5). However, the PARP domain of PARP12 was required to degrade ZIKV NS1 and NS3.

We found that ZIKV NS1 and NS3 protein abundance was increased after transfection with a PARP domain deletion construct when compared to transfection with full-length PARP12 (Fig. 3, B and C). The same truncation mutants were also transfected into HeLa cells that were subsequently infected with ZIKV to determine how the different deletions affected viral infection. Cells expressing full-length PARP12 or mutants lacking the ZnF or WWE domain showed similar rates of ZIKV infection, whereas cells expressing the mutant lacking the PARP domain showed increased ZIKV infection (Fig. 3E). In addition, treating A549 cells with increasing concentrations of the PARP enzyme inhibitors INO-1001 (3-aminobenzamide) or AG-014699 (rucaparib) increased viral replication (Fig. 3, F and G), without an impact on cell viability (Fig. 3, H and I). Thus, the PARP domain and its enzyme activity were essential to control ZIKV infection.

PARP12 limits NS1 and NS3 protein abundance by stimulating proteasome-mediated degradation

Because PARP12 did not affect the transcription of ZIKV *NS1* and *NS3* mRNA and the PARP domain was required for decreasing NS1 and NS3 proteins (Fig. 3, B and C), we hypothesized that it might decrease NS1 and NS3 at the protein abundance by altering protein stability and promoting degradation. We demonstrated that PARP12 could interact (Fig. 4A) and colocalize (Fig. 4B) with NS1 and NS3 proteins. When cells were cotransfected with plasmids encoding HA-PARP12 and His-NS1 or His-NS3, we found that treatment with the proteasome inhibitor MG132 reduced the degree of NS1 and NS3 protein decrease normally induced by PARP12 (Fig. 4, C and D). These data suggested that PARP12 mediated the degradation of NS1 and NS3 through the proteasome pathway.

Because proteasomes degrade proteins tagged by ubiquitin molecules, we evaluated whether PARP12 controlled ubiquitylation of NS1 and NS3. HEK293T cells were transfected with enhanced green fluorescent protein (EGFP)–PARP12, HA-ubiquitin, and either His-NS1 or His-NS3 plasmids. When NS1 and NS3 were immuno-precipitated and analyzed by immuno-blotting, cotransfection with PARP12 increased the ubiquitylation of NS1 and NS3 more than cotransfection with vector con trol (Fig. 4, E and F). In summary, these experiments demonstrate that PARP12 promotes degradation of ZIKV NS1 and NS3 proteins through the ubiquitin-proteasome pathway.

PARP12-associated degradation of ZIKV NS1 and NS3 requires its ADP-ribosylation activity

Proteins carrying a PARP domain can catalyze the ADP-ribosylation of their targets (24, 39). Subsequently, E3 ubiquitin ligases that recognize PARP proteins and the poly(ADP-ribose) on their bound targets direct ubiquitylation and proteasomal degradation of their targets (38, 41). Therefore, we tested whether ubiquityla tion and proteasomal degradation of NS1 and NS3 proteins resulted from ADP-ribosylation mediated by PARP12 and were dependent on their PARP enzyme activity. When HEK293T cells were cotransfected with plasmids encoding EGFP-PARP12 and His-NS1 or His-NS3, we found that PARP12 increased ADP-ribosylation of NS1 and NS3 (Fig. 5, A and B). Because the Gly[565] within the PARP domain of human PARP12 binds the amide group of NAD^+, which is essential for mono-ADP-ribosylation (MAR) activity (32, 39), we mutated PARP12 at that site (PARP12 G565A) to

impair its PARP enzyme activity (Fig. 5C). When PARP12 WT, PARP12 G565A, or empty vector were cotransfected with His-NS1 or NS3 into *PARP12^{-/-}* HEK293T cells, we found that ADP-ribosylation of NS1 and NS3 decreased when PARP12 G565A was transfected (Fig. 5, D and E). These data also confirmed the impaired PARP enzyme activity of the PARP12 G565A mutant. Evaluating ubiquitylation of immuno-precipitated NS1 and NS3 in *PARP12^{-/-}* HEK293T cells cotransfected with PARP12 WT, PARP12 G565A, or empty vector and HA-ubiquitin, His-NS1, or His-NS3 indicated that PARP12 WT enhanced the PAR and ubiquitylation of NS1 and NS3 proteins. However, the inactive PARP12 mutant (PARP12 G565A) neither poly-ADP-ribosylated nor ubiquitinated ZIKV NS1 and NS3 proteins (Fig. 5, D to G). In addition, the protein abundance of NS1 and NS3 was higher in cells expressing PARP12 G565A than in cells expressing PARP12 WT and was comparable to that in cells expressing vector control (Fig. 5, H and I), suggesting that PARP12 G565A was not as effective as PARP12 WT at triggering the ubiquitylation and degradation of NS1 and NS3. Consistently, overexpression of PARP12 G565A in HeLa cells did not suppress ZIKV replication as efficiently as PARP12 WT (Fig. 5J). Together, these results indicate that PARP12-mediated degradation of ZIKV NS1 and NS3 proteins requires its PARP enzyme activity.

After PARP12-mediated PAR, ZIKV NS1 and NS3 proteins are ubiquitinated on K48 and degraded by proteasome

Ubiquitin can bind to its substrates through its lysine residue at position 63 (Lys^{63} or K63) for modifications related to signal transduction, DNA repair, and protein activity, whereas modifications related to protein stability and degradation occur on Lys^{48} (K48). To distinguish the two, we cotransfected HEK293T cells with EGFP-PARP12, His-NS1, or His-NS3 and plasmids encoding versions of ubiquitin capable of binding substrate only through either K48 or K63. We observed that the ubiquitylation of NS1 and NS3 mediated by PARP12 was exclusively through K48 (Fig. 6, A and B) and not through K63 linkage (Fig. 6, C and D). These experiments demonstrate that PARP12 mediates the K48-linked ubiquitylation of ZIKV NS1 and NS3 proteins to promote their degradation through the ubiquitin-proteasome pathway. These results are consistent with our proposed model of how PARP12 interacts with ZIKV NS1 and NS3 proteins to initiate a cascade of events leading to their proteolysis (Fig. 6E). Our data indicate that PAR mediated by the PARP enzyme activity of PARP12 is crucial for the degradation of NS1 and NS3 proteins and control of ZIKV replication.

DISCUSSION

We have confirmed that *PARP12* is a functional ISG that restricts ZIKV infection. Although the antiviral properties of PARP12 have been previously reported (31, 33), the un derlying mechanism has been unclear. We demonstrated that PARP12 suppressed ZIKV replication through PARP domain–mediated PAR and subsequent proteasomal degradation of NS1 and NS3 proteins, which are critical for the virus's replication and immune evasion abilities. Although the related PARP isoform PARP13 specifically binds to retroviral RNA stimulating its degradation (26), in our study, we found that PARP12 decreased the ZIKV NS1 and NS3 protein abundance and that this effect was not through the inhibition of viral

mRNA transcription (Fig. 3D). The ability of PARP13 to directly target viral and host transcripts for degradation is primarily mediated by its ZnF domains (35, 42). However, despite having four CCCH-type ZnF motifs that are homologous to those of PARP13 (fig. S5), we found that the ZnF domains were not necessary for PARP12 to mediate its effect on ZIKV suppression (Fig. 3, B to D). Instead, the PARP domain of PARP12 appeared to play a role (Fig. 3, B, C, and E). Here, we described the critical functions of the PARP domains of PARP12 in post translational modification of ZIKV NS1 and NS3 proteins. Although we think that the ZnF domains of PARP12 are unnecessary in the degradation of NS1 and NS3, this does not exclude the possibility that they may contribute to ZIKV suppression by some other mechanism.

ADP-ribosylation is catalyzed by PARP enzyme activity. PARPs can modify their targets through either MAR or PAR (39). Some E3 ligases, such as TRIM25 and RNF146, can be recruited as PAR-binding proteins (40, 41, 43). E3 ligase–mediated, PAR-dependent ubiquitylation, which results in proteasomal degradation of target proteins, is carried out by multiple PARP proteins (38, 44). In our results, PARP12 promoted the ubiquitylation and proteasomal degradation of NS1 and NS3 in a manner dependent on its PARP enzyme activity, suggesting an indispensable and prerequisite role of ADP-ribosylation during this process. Although PARP12 belongs to the MAR sub-family (39), our results showed that NS1 and NS3 were poly-ADP-ribosylated by PARP12 (Fig. 5, A and B). Because the most kinetically impaired step in PAR is the initial MAR of a target protein (45, 46), the PARP12-catalyzed MAR reaction is likely the rate-limiting step of PAR. Other PARPs with PAR ability may extend the MAR initially performed by PARP12 to poly-ADP-ribosylate NS1 and NS3. The exact identity of this is still unclear, and this process may involve interplay between multiple PARP proteins.

PARP12 has activity against several other viruses, such as vesicular stomatitis virus (VSV), murine gammaherpes virus (MHV-68), and Venezuelan equine encephalitis virus (VEEV) (31, 33). This study adds ZIKV to that list and proposes a mechanism to explain how ZIKV replication is inhibited by this ISG. Our model system that measures viral protein levels in infected PARP12-overexpressing A549 cells could potentially be used to uncover the specific targets and mechanisms underlying PARP12's antiviral functions against other related flaviviruses, such as DENV, HCV (hepatitis C virus), or WNV. PARP12 has also been associated with the activation of nuclear factor κB and regulation of protein translation (32). These processes may present other means through which PARP12 inhibits viral replication. Together, our work highlights the unique antiviral mechanism of PARP12 and suggests that PARP agonists may have clinical utility when repurposed as ZIKV treatments.

MATERIALS AND METHODS

Virus, cells, and reagents

ZIKV strain GZ01/2016 (GenBank accession number KU820898) was used at a multiplicity of infection (MOI) of 0.1 in this study, except where indicated otherwise (47). MEF cells were isolated from GD14.5 Balb/c mice. The *IFNAR1*$^{-/-}$ A549 cell line was generated as described (20). A549, BHK-21, Vero, HeLa, and HEK293T cells were purchased from American Type Culture Collection and cultured in Dulbecco's modified Eagle's medium

(DMEM) (37°C, 5% CO_2) supplemented with 10% fetal bovine serum (FBS; 100 U/ml), penicillin, and streptomycin (50 μg/ml). INO-1001 (S1132) and AG-014699 (S1098) were purchased from Selleck. MG132 (M8699) was purchased from Sigma-Aldrich, and NITD008, an adenosine nucleoside analog inhibitor that inhibits the RdRp (RNA-dependent RNA polymerase) activity of *Flavivirus* (48), was a gift from P.-Y. Shi (Novartis Institute for Infectious Diseases).

Plaque assay

BHK-21 cells were seeded in a 12-well plate for 12 hours. Cells were washed with 1× PBS once and infected with virus samples for 1 hour. The culture supernatant was aspirated and replaced with DMEM containing 1% low-melting agarose and 2% FBS. Viral plaques were stained and counted 4 days after infection. The titer of ZIKV was quantified by plaque assay and normalized to WT control.

ZIKV binding, entry, and replicon assay

ZIKV cell binding and entry experiments were performed on the basis of the protocol described previously (34). Briefly, for the virus-binding assay, 2×10^5 cells were seeded in a 12-well plate and cultured for 24 hours, followed by infection with ZIKV (MOI = 2) and incubation at 4°C for 1 hour. Unbound virus was removed, cells were washed with 1× PBS twice, and then, cell lysates were harvested to determine the amount of viral RNA by qRT-PCR. For the entry assay, after binding at 4°C for 1 hour, the infected cells were washed with 1× PBS twice, followed by incubation with prewarmed DMEM for 10 min at 37°C. Subsequently, cells were rinsed three times with 1× PBS, then treated with 0.25% trypsin for 10 min, and again washed three times with 1× PBS. Total cellular RNA was extracted to quantify viral RNA by qRT-PCR.

A SZ01 ZIKV replicon carrying the seven ZIKV nonstructural proteins and *RLuc* gene was developed as described (49). A replicon assay was performed as previously published (49, 50), with minor modifications. Briefly, 2×10^5 BHK-21 cells in a 24-well plate were transfected with 200 ng of the in vitro–transcribed replicon containing the seven ZIKV nonstructural proteins and the *RLuc* reporter and with 200 ng of pMOI-PARP12 or control plasmid using a Lipofectamine 3000 reagent (Thermo Fisher Scientific). The cell lysates were collected after 48 hours, and the *RLuc* activity was measured using the *Renilla* Luciferase Assay system (Promega) in a GloMax 96 microplate luminometer.

DNA constructs

pMOI-GFP and pMOI-PARP12 (*Homo sapiens*) expression plasmids were purchased from GeneCopoeia and described previously (51). The viral RNA of the GZ01/2016 strain was isolated and used in reverse transcription PCR experiments to obtain the complementary DNA (cDNA) sequences of ZIKV nonstructural proteins (NS1, NS2A, NS2B, NS3, NS4A, NS4B, and NS5). Each ZIKV nonstructural gene was cloned into the pcDNA6/V5-His A expression vector (Invitrogen) using standard molecular cloning techniques and verified by sequencing. DsRed-NS1, DsRed-NS3, HA- or EGFP-PARP12, and PARP12 mutants were cloned using standard molecular cloning and oligo-nucleotide mutagenesis methods. HA-ubiquitin, HA-K48, and HAK63 plasmids were provided by S. Wang (52). Briefly, WT,

K48, and K63 ubiquitin were cloned into pCMV-HA vector to generate HA-ubiquitin, which was subsequently mutated at the indicated residue to generate HA-K48 and HA-K63 plasmids. To create a stable cell line for PARP12 expression, PARP12 was cloned into the pMXsIG-IgkFLAG vector and cotransfected into A549 and MEF cells with VSV glyco-protein and pCpG helper plasmids. The cells were collected 72 hours after transfection, and the PARP12-overexpressing cells were then sorted by fluorescence-activated cell sorting (FACS).

Immunoblotting

WT and *PARP12*$^{-/-}$ HEK293T cells were cotransfected with the plasmids listed in the main text and, where indicated, were treated with 10 μM MG132 (Sigma-Aldrich) for 10 hours. Twenty-eight hours after transfection, cells were treated with lysis buffer [50 mM tris-HCl (pH 7.5), 150 mM NaCl, 5 mM EDTA, 1% NP-40, 1 mM phenylmethylsulfonyl fluoride (PMSF), and 1× protease inhibitor (Roche)]. The cell extracts were immunoblotted with the indicated antibodies to measure the level of the expressed proteins. Mouse anti–β-actin (ZSGB-Bio), rabbit anti-GFP (Abcam), mouse anti-poly(ADP-ribose) (GeneTex), rabbit anti-PARP12 (Sigma-Aldrich), mouse anti-ZIKV NS1 (Abcam), rabbit anti-ZIKV NS3 (GeneTex), and mouse anti-HA, anti-His, and anti-Flag tag antibodies (Sigma-Aldrich) were used for detection at the appropriate dilutions. Quantification of Western blot results was normalized to actin or correspondingly input control and pooled from three independent experiments.

Immunoprecipitation and coimmunoprecipitation

HEK293T cells were transfected by the indicated plasmids. Thirty hours after transfection, protein was extracted using solution A [50 mM tris-HCl (pH 7.5), 150 mM NaCl, 5 mM EDTA, 1% Triton X-100, 1 mM PMSF, and 1× protease inhibitor (Roche)]. An aliquot of the extracts was immunoblotted with the indicated antibodies. The remaining extracts were immunoprecipitated using Sepharose beads bound to anti-His or anti-HA antibodies (Sigma-Aldrich) at 4°C overnight. After washing the Sepharose beads four times with solution B [50 mM tris-HCl (pH 7.5), 150 mM NaCl, 0.2% Triton X-100, and 1 mM PMSF], proteins were eluted by heating the beads to 98°C in 1× SDS–polyacrylamide gel electrophoresis loading buffer [50 mM tris-HCl (pH 6.8), 2% (v/v) SDS, 6% (v/v) glycerol, and 2% (v/v) β-mercaptoethanol]. The eluate was analyzed by immunoblotting with the indicated antibodies.

Gene knockout by the CRISPR/Cas9 system

To knockout ISGs in the A549 cell line, for each ISG, two small guide RNAs (sgRNAs) (~100–base pair gap sequence) targeting the gene were designed and cloned into sgRNA expression vectors under the control of the U6 promoter (table S1). A549 cells were cotransfected with sgRNAs and Cas9 expression plasmids, followed by puromycin selection, as described previously (53, 54). Single clones were isolated by FACS and confirmed by PCR genotyping and sequencing. *PARP12*$^{-/-}$ HEK293T and MEF (sgRNAs target murine *PARP12*) were generated by the same method.

RNA isolation, reverse transcription, and qRT-PCR

Total RNA from cells or viruses was extracted with the PureLink RNA Extraction kit (Thermo Fisher Scientific). Viral RNA copies were measured by qRT-PCR (55) with the One Step PrimeScript RT-PCR kit (TaKaRa). ZIKV primers and TaqMan probes were described previously (56). Primers used to amplify corresponding genes were obtained from PrimerBank (https://pga.mgh.harvard.edu/primerbank/) and listed as follows: *PARP12*, 5′-TTTCAAAGCCTTCGTTCAGA-3′ (forward) and 5′-TTGGTATTGCAGGTTTGCAT-3′ (reverse); GZ01/2016 strain *NS1*, 5′-GATGCGGTACAGGGGTGTTT-3′ (forward) and 5′-CCCGCAGATACCATCTTCCC-3′ (reverse); *NS3*, 5′-CTGAGGCCGACAAAGTAGCA-3′ (forward) and 5′-CCGGCAGATGCAACCTGATA-3′ (reverse); *GAPDH*, 5′-CTGGGCTACACTGAGCACC-3′ (forward) and 5′-AAGTGGTCGTTGAGGGCAATG-3′ (reverse). SYRB Green qPCR mix (TransGen Biotech) was used to analyze mRNA levels on an ABI 7500 (Applied Biosystems) analyzer.

Immunofluorescence staining and confocal imaging

Vero cells were seeded in a confocal dish (Solarbio) and transfected with EGFP-PARP12 and DsRed-NS1 or NS3 plasmids. After 24 hours, cells were fixed with 4% paraformaldehyde for 15 min and permeabilized in 0.2% Triton X-100 for 15 min at room temperature. The cells were washed three times with PBS. Nuclei were stained with 4′,6-diamidino-2-phenylindole (Thermo Fisher Scientific). Cells were imaged on an LSM 700 (Carl Zeiss) confocal microscope, and the images were analyzed with Imaris and ImageJ software.

Statistical analysis

All data were analyzed using Prism software (GraphPad). Statistical evaluation was performed by two-way Student's *t* test. Data are means ± SEM, and *P* values are indicated by *$P < 0.5$, **$P < 0.01$, and ***$P < 0.001$. All cellular experiments were repeated at least three times.

Supplementary Material

Refer to Web version on PubMed Central for supplementary material.

Acknowledgments:

REFERENCES

1. Campos GC, Sardi SI, Sarno M, Brites C, Zika virus infection, a new public health challenge. Braz. J. Infect. Dis 20, 227–228 (2016). [PubMed: 27215946]

2. Ong CW, Zika virus: An emerging infectious threat. Intern. Med. J 46, 525–530 (2016). [PubMed: 27170237]

3. Cauchemez S, Besnard M, Bompard P, Dub T, Guillemette-Artur P, Eyrolle-Guignot D, Salje H, Van Kerkhove MD, Abadie V, Garel C, Fontanet A, Mallet H-P, Association between Zika virus and microcephaly in French Polynesia, 2013–2015: A retrospective study. Lancet 387, 2125–2132 (2016). [PubMed: 26993883]

4. França GV, Schuler-Faccini L, Oliveira WK, Henriques CM, Carmo EH, Pedi VD, Nunes ML, Castro MC, Serruya S, Silveira MF, Barros FC, Victora CG, Congenital Zika virus syndrome in Brazil: A case series of the first 1501 livebirths with complete investigation. Lancet 388, 891–897 (2016). [PubMed: 27372398]

5. Bearcroft WG, Zika virus infection experimentally induced in a human volunteer. Trans. R. Soc. Trop. Med. Hyg 50, 442–448 (1956). [PubMed: 13380987]

6. Fauci AS, Morens DM, Zika virus in the Americas—Yet another arbovirus threat. N. Engl. J. Med 374, 601–604 (2016). [PubMed: 26761185]

7. Simpson DIH, Zika virus infection in man. Trans. R. Soc. Trop. Med. Hyg 58, 335–338 (1964). [PubMed: 14175744]

8. Ximenes ASFC, Pires P, Werner H, Jungmann PM, Rolim Filho EL, Andrade EP, Lemos RS, Peixoto AB, Zare Mehrjardi M, Tonni G, Araujo Júnior E, Neuroimaging findings using transfontanellar ultrasound in newborns with microcephaly: A possible association with congenital Zika virus infection. J. Matern. Fetal Neonatal Med 1–9 (2017).

9. Li C, Xu D, Ye Q, Hong S, Jiang Y, Liu X, Zhang N, Shi L, Qin CF, Xu Z, Zika virus disrupts neural progenitor development and leads to microcephaly in mice. Cell Stem Cell 19, 672 (2016). [PubMed: 27814481]

10. Miner JJ, Cao B, Govero J, Smith AM, Fernandez E, Cabrera OH, Garber C, Noll M, Klein RS, Noguchi KK, Mysorekar IU, Diamond MS, Zika virus infection during pregnancy in mice causes placental damage and fetal demise. Cell 165, 1081–1091 (2016). [PubMed: 27180225]

11. Kostyuchenko VA, Lim EXY, Zhang S, Fibriansah G, Ng T-S, Ooi JS, Shi J, Lok S-M, Structure of the thermally stable Zika virus. Nature 533, 425–428 (2016). [PubMed: 27093288]

12. Akey DL, Brown WC, Dutta S, Konwerski J, Jose J, Jurkiw TJ, DelProposto J, Ogata CM, Skiniotis G, Kuhn RJ, Smith JL, Flavivirus NS1 structures reveal surfaces for associations with membranes and the immune system. Science 343, 881–885 (2014). [PubMed: 24505133]

13. Edeling MA, Diamond MS, Fremont DH, Structural basis of flavivirus NS1 assembly and antibody recognition. Proc. Natl. Acad. Sci. U.S.A 111, 4285–4290 (2014). [PubMed: 24594604]

14. Leung JY, Pijlman GP, Kondratieva N, Hyde J, Mackenzie JM, Khromykh AA, Role of nonstructural protein NS2A in flavivirus assembly. J. Virol 82, 4731–4741 (2008). [PubMed: 18337583]

15. Liu WJ, Wang XJ, Clark DC, Lobigs M, Hall RA, Khromykh AA, A single amino acid substitution in the West Nile virus nonstructural protein NS2A disables its ability to inhibit alpha/beta interferon induction and attenuates virus virulence in mice. J. Virol 80, 2396–2404 (2006). [PubMed: 16474146]

16. Sironi M, Forni D, Clerici M, Cagliani R, Nonstructural proteins are preferential positive selection targets in Zika virus and related flaviviruses. PLOS Negl. Trop. Dis 10, e0004978 (2016). [PubMed: 27588756]

17. Schoggins JW, Wilson SJ, Panis M, Murphy MY, Jones CT, Bieniasz P, Rice CM, A diverse range of gene products are effectors of the type I interferon antiviral response. Nature 472, 481–485 (2011). [PubMed: 21478870]

18. Schoggins JW, Rice CM, Interferon-stimulated genes and their antiviral effector functions. Curr. Opin. Virol 1, 519–525 (2011). [PubMed: 22328912]

19. Hamel R, Dejarnac O, Wichit S, Ekchariyawat P, Neyret A, Luplertlop N, Perera-Lecoin M, Surasombatpattana P, Talignani L, Thomas F, Cao-Lormeau V-M, Choumet V, Briant L, Desprès P,

Amara A, Yssel H, Missé D, Biology of Zika virus infection in human skin cells. J. Virol 89, 8880–8896 (2015). [PubMed: 26085147]

20. Li C, Deng Y-Q, Wang S, Ma F, Aliyari R, Huang X-Y, Zhang N-N, Watanabe M, Dong H-L, Liu P, Li X-F, Ye Q, Tian M, Hong S, Fan J, Zhao H, Li L, Vishlaghi N, Buth JE, Au C, Liu Y, Lu N, Du P, Qin FX-F, Zhang B, Gong D, Dai X, Sun R, Novitch BG, Xu Z, Qin C-F, Cheng G, 25-Hydroxycholesterol protects host against Zika virus infection and its associated microcephaly in a mouse model. Immunity 46, 446–456 (2017). [PubMed: 28314593]

21. Hottiger MO, Hassa PO, Lüscher B, Schüler H, Koch-Nolte F, Toward a unified nomenclature for mammalian ADP-ribosyltransferases. Trends Biochem. Sci 35, 208–219 (2010). [PubMed: 20106667]

22. Gibson BA, Kraus WL, New insights into the molecular and cellular functions of poly(ADP-ribose) and PARPs. Nat. Rev. Mol. Cell Biol 13, 411–424 (2012). [PubMed: 22713970]

23. Aravind L, Zhang D, de Souza RF, Anand S, Iyer LM, The natural history of ADP-ribosyltransferases and the ADP-ribosylation system. Curr. Top. Microbiol. Immunol 384, 3–32 (2015). [PubMed: 25027823]

24. Kuny CV, Sullivan CS, Virus–host interactions and the ARTD/PARP family of enzymes. PLOS Pathog. 12, e1005453 (2016). [PubMed: 27010460]

25. Smulson ME, Simbulan-Rosenthal CM, Boulares AH, Yakovlev A, Stoica B, Iyer S, Luo R, Haddad B, Wang ZQ, Pang T, Jung M, Dritschilo A, Rosenthal DS, Roles of poly(ADP-ribosyl)ation and PARP in apoptosis, DNA repair, genomic stability and functions of p53 and E2F-1. Adv. Enzyme Regul 40, 183–215 (2000). [PubMed: 10828352]

26. Gao G, Guo X, Goff SP, Inhibition of retroviral RNA production by ZAP, a CCCH-type zinc finger protein. Science 297, 1703–1706 (2002). [PubMed: 12215647]

27. Grady SL, Hwang J, Vastag L, Rabinowitz JD, Shenk T, Herpes simplex virus 1 infection activates poly(ADP-ribose) polymerase and triggers the degradation of poly(ADP-ribose) glycohydrolase. J. Virol 86, 8259–8268 (2012). [PubMed: 22623791]

28. Guzyk MM, Tykhomyrov AA, Nedzvetsky VS, Prischepa IV, Grinenko TV, Yanitska LV, Kuchmerovska TM, Poly(ADP-ribose) polymerase-1 (PARP-1) inhibitors reduce reactive gliosis and improve angiostatin levels in retina of diabetic rats. Neurochem. Res 41, 2526–2537 (2016). [PubMed: 27255598]

29. Yu M, Zhang C, Yang Y, Yang Z, Zhao L, Xu L, Wang R, Zhou X, Huang P, The interaction between the PARP10 protein and the NS1 protein of H5N1 AIV and its effect on virus replication. Virol. J 8, 546 (2011). [PubMed: 22176891]

30. Atasheva S, Akhrymuk M, Frolova EI, Frolov I, New PARP gene with an anti-alphavirus function. J. Virol 86, 8147–8160 (2012). [PubMed: 22623789]

31. Atasheva S, Frolova EI, Frolov I, Interferon-stimulated poly(ADP-ribose) polymerases are potent inhibitors of cellular translation and virus replication. J. Virol 88, 2116–2130 (2014). [PubMed: 24335297]

32. Welsby I, Hutin D, Gueydan C, Kruys V, Rongvaux A, Leo O, PARP12, an interferon-stimulated gene involved in the control of protein translation and inflammation. J. Biol. Chem 289, 26642–26657 (2014). [PubMed: 25086041]

33. Liu S-Y, Sanchez DJ, Aliyari R, Lu S, Cheng G, Systematic identification of type I and type II interferon-induced antiviral factors. Proc. Natl. Acad. Sci. U.S.A 109, 4239–4244 (2012). [PubMed: 22371602]

34. Zhu X, He Z, Yuan J, Wen W, Huang X, Hu Y, Lin C, Pan J, Li R, Deng H, Liao S, Zhou R, Wu J, Li J, Li M, IFITM3-containing exosome as a novel mediator for anti-viral response in dengue virus infection. Cell. Microbiol 17, 105–118 (2015). [PubMed: 25131332]

35. Todorova T, Bock FJ, Chang P, PARP13 regulates cellular mRNA post-transcriptionally and functions as a pro-apoptotic factor by destabilizing TRAILR4 transcript. Nat. Commun 5, 5362 (2014). [PubMed: 25382312]

36. Guo X, Ma J, Sun J, Gao G, The zinc-finger antiviral protein recruits the RNA processing exosome to degrade the target mRNA. Proc. Natl. Acad. Sci. U.S.A 104, 151–156 (2007). [PubMed: 17185417]

37. Zhu Y, Wang X, Goff SP, Gao G, Translational repression precedes and is required for ZAP-mediated mRNA decay. EMBO J 31, 4236–4246 (2012). [PubMed: 23023399]

38. Wang Z, Michaud GA, Cheng Z, Zhang Y, Hinds TR, Fan E, Cong F, Xu W, Recognition of the iso-ADP-ribose moiety in poly(ADP-ribose) by WWE domains suggests a general mechanism for poly(ADP-ribosyl)ation-dependent ubiquitination. Genes Dev. 26, 235–240 (2012). [PubMed: 22267412]

39. Bock FJ, Chang P, New directions in PARP biology. FEBS J. 283, 4017–4031 (2016). [PubMed: 27087568]

40. Li MMH, Lau Z, Cheung P, Aguilar EG, Schneider WM, Bozzacco L, Molina H, Buehler E, Takaoka A, Rice CM, Felsenfeld DP, MacDonald MR, TRIM25 enhances the antiviral action of zinc-finger antiviral protein (ZAP). PLOS Pathog. 13, e1006145 (2017). [PubMed: 28060952]

41. Zhang Y, Liu S, Mickanin C, Feng Y, Charlat O, Michaud GA, Schirle M, Shi X, Hild M, Bauer A, Myer VE, Finan PM, Porter JA, Huang S-MA, Cong F, RNF146 is a poly(ADP-ribose)-directed E3 ligase that regulates axin degradation and Wnt signalling. Nat. Cell Biol 13, 623–629 (2011). [PubMed: 21478859]

42. Guo X, Carroll J-WN, Macdonald MR, Goff SP, Gao G, The zinc finger antiviral protein directly binds to specific viral mRNAs through the CCCH zinc finger motifs. J. Virol 78, 12781–12787 (2004). [PubMed: 15542630]

43. DaRosa PA, Wang Z, Jiang X, Pruneda JN, Cong F, Klevit RE, Xu W, Allosteric activation of the RNF146 ubiquitin ligase by a poly(ADP-ribosyl)ation signal. Nature 517, 223–226 (2015). [PubMed: 25327252]

44. Aravind L, The WWE domain: A common interaction module in protein ubiquitylation and ADP ribosylation. Trends Biochem. Sci 26, 273–275 (2001). [PubMed: 11343911]

45. Mao Z, Hine C, Tian X, Van Meter M, Au M, Vaidya A, Seluanov A, Gorbunova V, SIRT6 promotes DNA repair under stress by activating PARP1. Science 332, 1443–1446 (2011). [PubMed: 21680843]

46. Mendoza-Alvarez H, Alvarez-Gonzalez R, Poly(ADP-ribose) polymerase is a catalytic dimer and the automodification reaction is intermolecular. J. Biol. Chem 268, 22575–22580 (1993). [PubMed: 8226768]

47. Zhang F-C, Li X-F, Deng Y-Q, Tong Y-G, Qin C-F, Excretion of infectious Zika virus in urine. Lancet Infect. Dis 16, 641–642 (2016). [PubMed: 27184420]

48. Lo MK, Shi P-Y, Chen Y-L, Flint M, Spiropoulou CF, In vitro antiviral activity of adenosine analog NITD008 against tick-borne flaviviruses. Antiviral Res. 130, 46–49 (2016). [PubMed: 27016316]

49. Xie X, Zou J, Shan C, Yang Y, Kum DB, Dallmeier K, Neyts J, Shi P-Y, Zika virus replicons for drug discovery. EBioMedicine 12, 156–160 (2016). [PubMed: 27658737]

50. Liu Z-Y, Li X-F, Jiang T, Deng Y-Q, Zhao H, Wang H-J, Ye Q, Zhu S-Y, Qiu Y, Zhou X, Qin E-D, Qin C-F, Novel *cis*-acting element within the capsid-coding region enhances flavivirus viral-RNA replication by regulating genome cyclization. J. Virol 87, 6804–6818 (2013). [PubMed: 23576500]

51. Liu S-Y, Aliyari R, Chikere K, Li G, Marsden MD, Smith JK, Pernet O, Guo H, Nusbaum R, Zack JA, Freiberg AN, Su L, Lee B, Cheng G, Interferon-inducible cholesterol-25-hydroxylase broadly inhibits viral entry by production of 25-hydroxycholesterol. Immunity 38, 92–105 (2013). [PubMed: 23273844]

52. Wang S, Chen Y, Li C, Wu Y, Guo L, Peng C, Huang Y, Cheng G, Qin FX-F, TRIM14 inhibits hepatitis C virus infection by SPRY domain-dependent targeted degradation of the viral NS5A protein. Sci. Rep 6, 32336 (2016). [PubMed: 27578425]

53. Cong L, Ran FA, Cox D, Lin S, Barretto R, Habib N, Hsu PD, Wu X, Jiang W, Marraffini LA, Zhang F, Multiplex genome engineering using CRISPR/Cas systems. Science 339, 819–823 (2013). [PubMed: 23287718]

54. Mali P, Yang L, Esvelt KM, Aach J, Guell M, DiCarlo JE, Norville JE, Church GM, RNA-guided human genome engineering via Cas9. Science 339, 823–826 (2013). [PubMed: 23287722]

55. Johnson BW, Russell BJ, Lanciotti RS, Serotype-specific detection of dengue viruses in a fourplex real-time reverse transcriptase PCR assay. J. Clin. Microbiol 43, 4977–4983 (2005). [PubMed: 16207951]

56. Deng Y-Q, Zhao H, Li X-F, Zhang N-N, Liu Z-Y, Jiang T, Gu D-Y, Shi L, He J-A, Wang H-J, Sun Z-Z, Ye Q, Xie D-Y, Cao W-C, Qin C-F, Isolation, identification and genomic characterization of the Asian lineage Zika virus imported to China. Sci. China Life Sci 59, 428–430 (2016). [PubMed: 26993654]
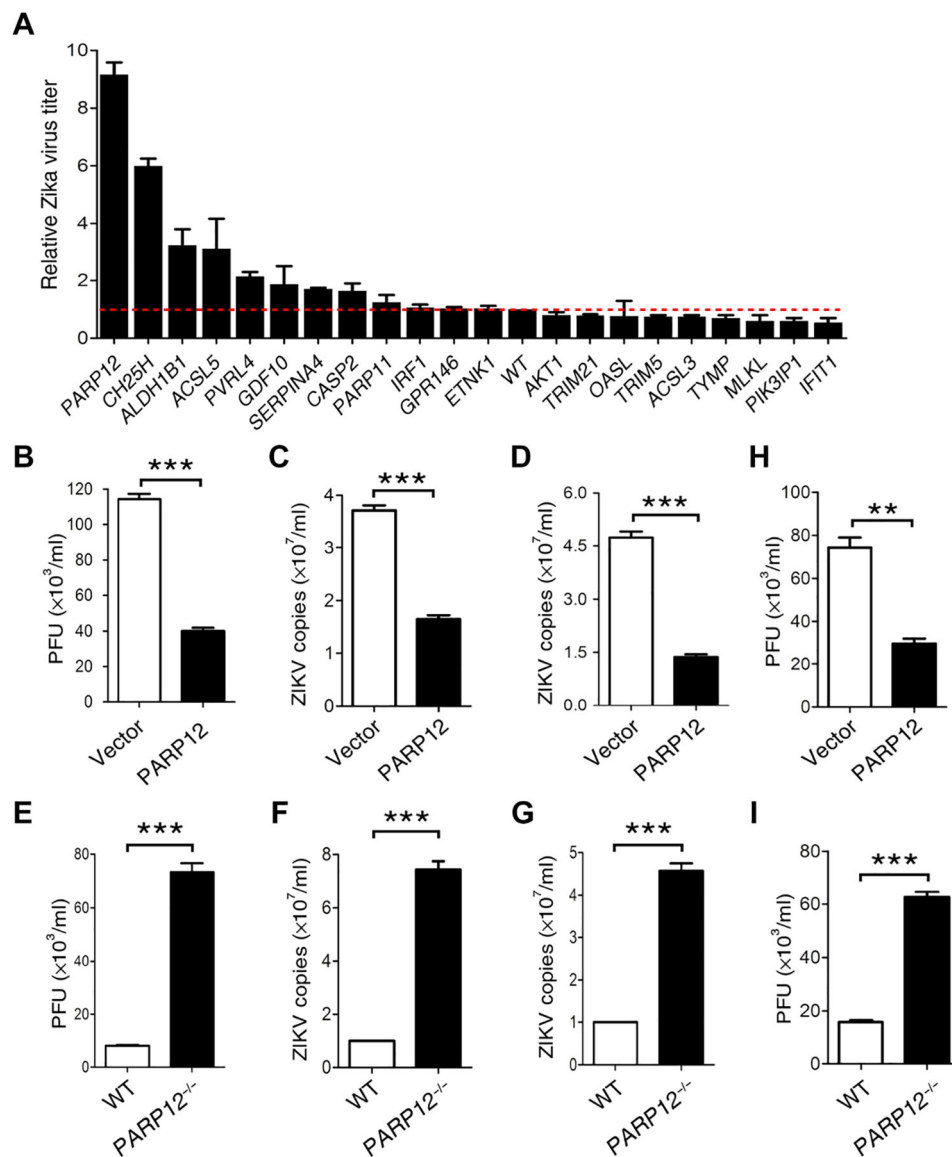
Fig. 1. ISG *PARP12* suppresses ZIKV replication in vitro.
(**A**) Individual ISGs were knocked out in A549 cells that were subsequently infected with ZIKV. Cell culture supernatants were collected at 24 hours after infection, and ZIKV titers were measured by plaque assay. (**B** to **D**) PARP12-overexpressing or control vector–transfected A549 cells were infected with ZIKV. Viral accumulation after 24 hours in the culture supernatants (B and C) and cell lysates (D) was measured by plaque assay (B) or qRT-PCR (C and D). PFU, plaque-forming units. (**E** to **G**) *PARP12*$^{-/-}$ and WT A549 cells were infected with ZIKV. Viral accumulation after 24 hours in the culture supernatants (E and F) and cell lysates (G) was measured by plaque assay (E) or qRT-PCR (F and G). (**H**) PARP12-overexpressing MEF cells were infected with ZIKV. Viral accumulation after 24 hours in the culture supernatants was measured by plaque assay. (**I**) *PARP12*$^{-/-}$ MEF cells were infected with ZIKV. Viral accumulation after 24 hours in the culture supernatants was

measured by plaque assay. Viral titers and RT-PCR data (A to I) are means ± SEM from three independent experiments. **$P < 0.01$ and ***$P < 0.001$ by Student's t test (B to I).

**Fig. 2. PARP12 suppresses ZIKV by reducing NS1 and NS3 protein abundance.**
(**A**) Control, PARP12-overexpressing, and *PARP12*^{−/−} A549 cells were incubated with ZIKV at 4°C for 1 hour and then washed extensively with phosphate-buffered saline (PBS). Cell surface binding was assessed by determining the viral copy number in the cell lysates by qRT-PCR. (**B**) Control, PARP12-overexpressing, and *PARP12*^{−/−} A549 cells were incubated with ZIKV at 4°C for 1 hour and then allowed to internalize bound ZIKV by incubation at 37°C for another 10 min. Viral entry into cells was assessed by determining the viral copy number in the cell lysates by qRT-PCR. (**C**) BHK-21 cells were cotransfected with either the PARP12 expression plasmid or empty vector and with RNA from a ZIKV replicon encoding an *RLuc* reporter. At 24 hours after transfection, luciferase activity in cell lysates was determined. NITD008 was used as a positive control. DMSO, dimethyl sulfoxide. (**D**) Western blot analysis of lysates from HEK293T cells cotransfected with plasmids encoding one of the ZIKV nonstructural proteins NS1/2B/3/4A/4B/5 and hemagglutinin (HA)–PARP12 or vector control. (**E**) Densitometry analysis of data in (D). (**F**) Western blot analysis of lysates from HEK293T cells cotransfected with plasmids

encoding one of the ZIKV His-NS1/3/4A and increasing amounts of HA-PARP12 plasmids (0, 100, 300, and 500 ng). (**G**) Densitometry analysis of data in (F). (**H**) Western blot analysis of lysates from WT and *PARP12*$^{-/-}$ HEK293T cells cotransfected with plasmids encoding ZIKV NS1 (top) or NS3 (bottom) and HA-PARP12 or vector control, as indicated. (**I**) Densitometry analysis of data in (H). (**J**) Western blot analysis of lysates from WT and *PARP12*$^{-/-}$ A549 cells infected with ZIKV for 24 hours. (**K**) Densitometry analysis of data in (J). RT-PCR and luciferase data (A to C) are means ± SEM from three independent experiments. Western blot results (D, F, H, and J) are representative of three independent experiments. Data (E, G, I, and K) are means ± SEM pooled from three independent experiments. **$P < 0.01$ and ***$P < 0.001$ by Student's *t* test.
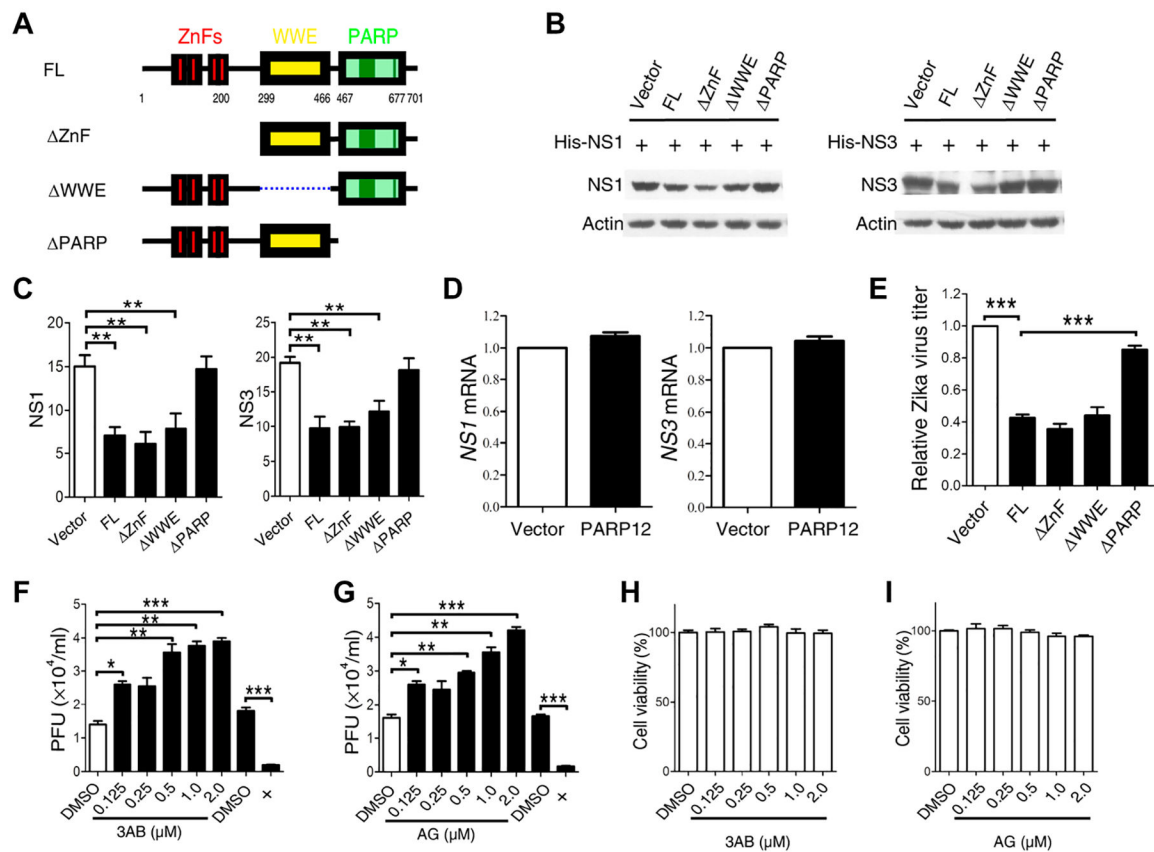
Fig. 3. The PARP domain of PARP12 is required to reduce NS1 and NS3 protein abundance.
(**A**) Map of the functional regions of full-lenght (FL) PARP12 and deletion constructs. (**B**) Western blot analysis of lysates from *PARP12*−/− HEK293T cells cotransfected as indicated with His-tagged NS1 or NS3 and the PARP12-deletion constructs. (**C**) Densitometry analysis of data in (B). (**D**) qRT-PCR analysis of *NS1* and *NS3* mRNA expression in HEK293T cells at 24 hours after cotransfection with either His-NS1 or His-NS3 and with PARP12 or control plasmids. (**E**) Viral replication was assessed by plaque assay of cell culture supernatants taken 24 hours after HeLa cells transfected with PARP12 truncated mutants or control plasmids were infected by ZIKV. (**F** and **G**) Viral replication was assessed by plaque assay of cell culture super natants taken 49 hours after A549 cells were infected with ZIKV for 1 hour and then treated with INO-1001 [3-aminobenzamide (3AB)] (F) or AG-014699 (AG; rucaparib) (G) at the indicated concentrations. NITD008 was used as a positive control. (**H** and **I**) Cell viability was assessed by MTT assay of A549 cells pretreated with indicated concentration of INO-1001 (3-aminobenzamide) (H) and AG-014699 (rucaparib) (I) for 48 hours. Data were normalized to DMSO control. Western blot results (B) are representative of three independent experiments. Data (C to I) are means ± SEM from three independent experiments. *$P < 0.05$, **$P < 0.01$, and ***$P < 0.001$ by Student's *t* test.
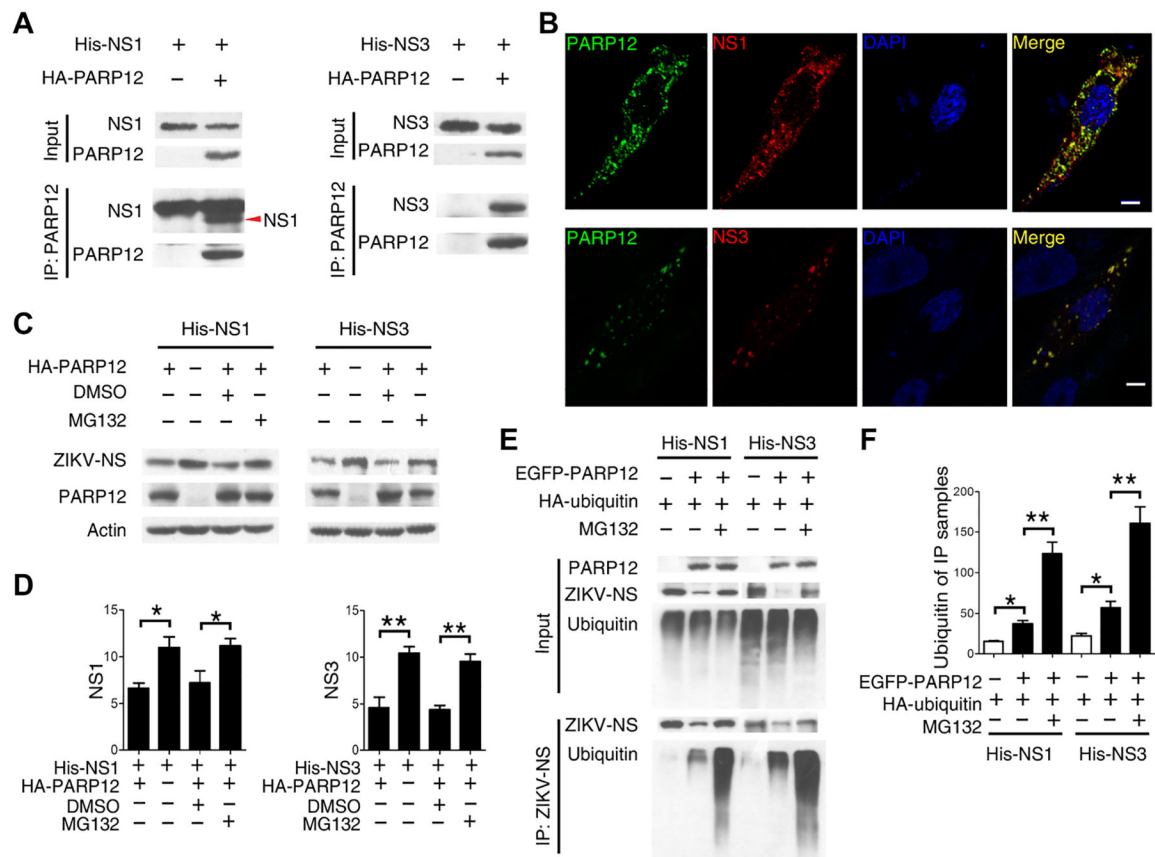
Fig. 4. PARP12 reduces NS1 and NS3 protein abundance through proteasomal degradation.
(**A**) Western blot analysis of lysates immunoprecipitated (IP) for PARP12 from HEK293T cells co transfected with HA-PARP12 and His-NS1 or His-NS3 plasmids. (**B**) Confocal microscopy analysis of Vero cells that were cotransfected with EGFP-PARP12 and DsRed-NS1 or DsRed-NS3 plasmids. Scale bars, 5 μm. (**C**) Western blot analysis of lysates from HEK293T cells cotransfected with HA-PARP12 and His-NS1 or His-NS3, as indicated. After 18 hours, cells were treated with 10 μM MG132 for 10 hours, where indicated. (**D**) Densitometry analysis of data in (C). (**E**) Western blot analysis of lysates immuno-precipitated for His-tagged proteins from HEK293T cells cotransfected with HA-ubiquitin, EGFP-PARP12, and His-NS1 or His-NS3 plasmids and treated with MG132, as indicated. (**F**) Densitometry analysis of data in (E). Western blot (A, C, and E) and confocal (B) results are representative of three independent experiments. Data (D and F) are means ± SEM pooled from three independent experiments. *$P < 0.05$ and **$P < 0.01$ by Student's t test.
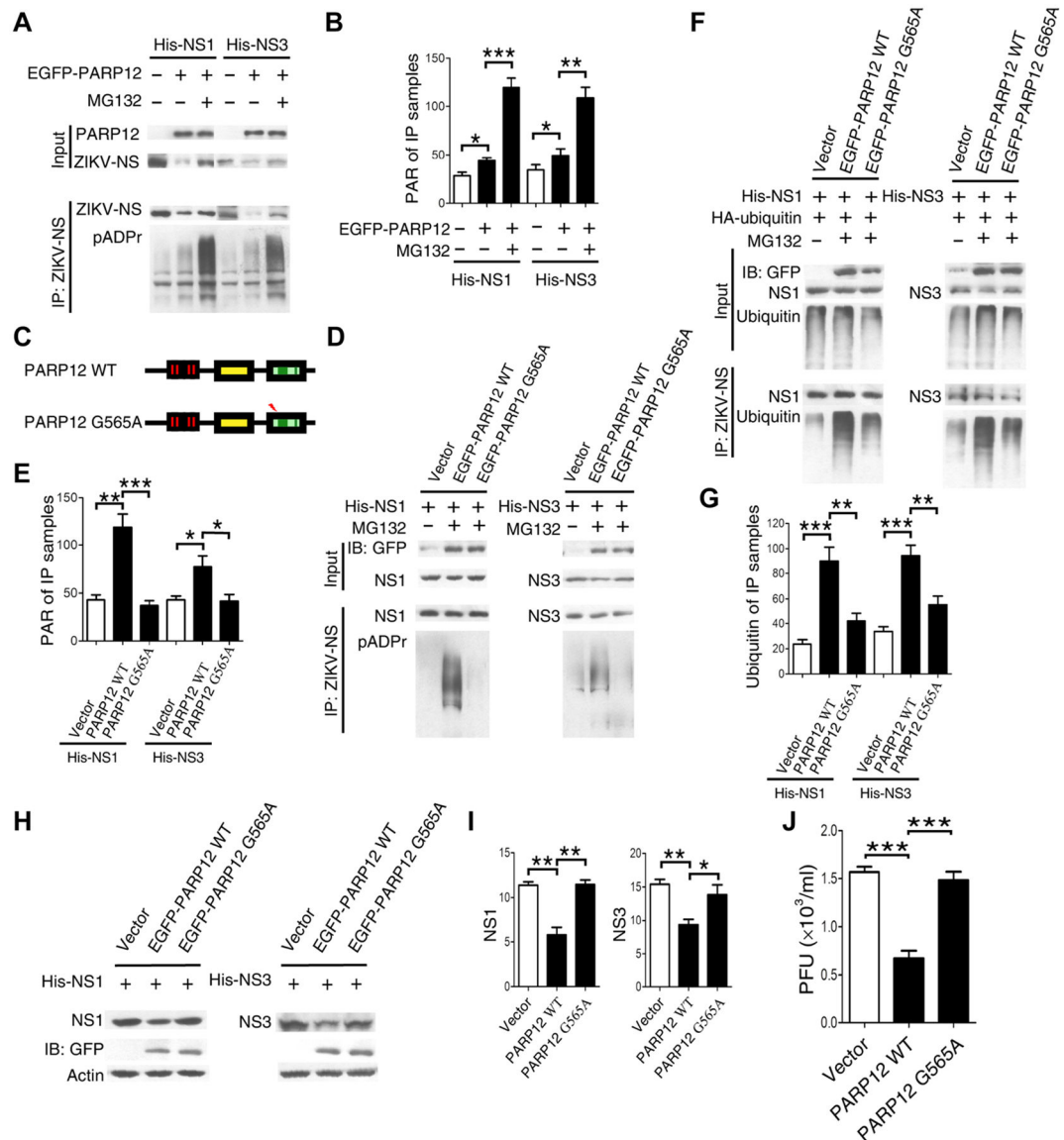
Fig. 5. Degradation of NS1 and NS3 protein is dependent on PARP12 ADP-ribosylation activity.
(**A**) Western blot analysis of lysates immunoprecipitated for His-tagged proteins from HEK293T cells transfected with EGFP-PARP12 and His-NS1 or His-NS3 plasmids and treated with MG132, as indicated. (**B**) Densitometry analysis of data in (A). (**C**) Map of the functional regions of WT and G565A PARP12 constructs. A PARP12 mutant with a disruption in the catalytic site (G565A) was generated by site-directed PCR mutagenesis. (**D**) Western blot analysis of lysates immunoprecipitated for His-tagged proteins from *PARP12*$^{-/-}$ HEK293T cells transfected with His-NS1 or His-NS3 and with EGFP-PARP12 WT, EGFP-PARP12 G565A, or vector control plasmids. (**E**) Densitometry analysis of data in (D). (**F**) Western blot analysis of lysates immunoprecipitated for His-tagged proteins from *PARP12*$^{-/-}$ HEK392T cells cotransfected with HA-ubiquitin and His-NS1 or NS3 plasmids, as well as EGFP-PARP12 WT, EGFP-PARP12 G565A, or vector control plasmid constructs. (**G**) Densitometry analysis of data in (F). (**H**) Western blot analysis of lysates from

PARP12^{−/−} HEK392T cells cotransfected with His-NS1 or His-NS3 and with EGFP-PARP12 WT, EGFP-PARP12 G565A, or vector control plasmids. (**I**) Densitometry analysis of data in (H). (**J**) Viral replication was assessed by plaque assay of cell culture supernatants taken 24 hours after HeLa cells transfected with EGFP-PARP12 WT, EGFP-PARP12 G565A, or vector control plasmids were infected with ZIKV. Western blots (A, D, F, and H) are representative of three independent experiments. Data (B, E, G, and I) and viral titers (J) are means ± SEM pooled from three independent experiments. *$P < 0.05$, **$P < 0.01$, and ***$P < 0.001$ by Student's *t* test.
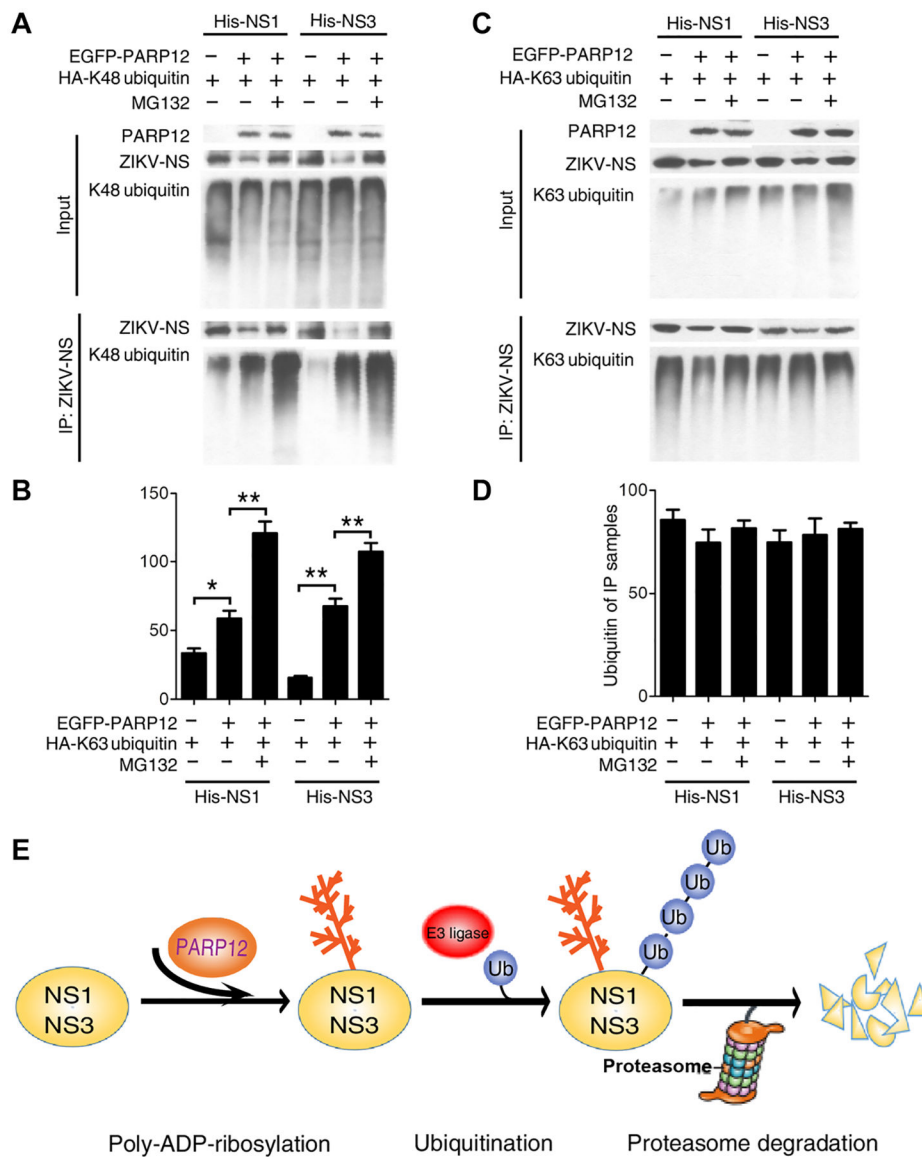
Fig. 6. After PARP12-mediated PAR, ZIKV NS1 and NS3 proteins are ubiquitinated on K48 and degraded.

(**A**) Western blot analysis of lysates immunoprecipitated for His-tagged proteins from HEK293T cells were cotransfected with EGFP-PARP12, His-NS1 or His-NS3, and HA-K48 ubiquitin mutants. MG132 was added as indicated. (**B**) Densitometry analysis of the data in (A). (**C**) Western blot analysis of lysates immunoprecipitated for His-tagged proteins from HEK293T cells were cotransfected with EGFP-PARP12, His-NS1 or His-NS3, and HA-K63 ubiquitin mutants. MG132 was added as indicated. (**D**) Densitometry analysis of the data in (C). (**E**) PARP12 mediates PAR of NS1 and NS3, which are subsequently ubiquitinated by an E3 ligase that is recruited by the PAR modification. Ubiquitinated NS1 and NS3 are then recognized and targeted by the proteasome for degradation. Western blot results (A and C) are representative of three independent experiments. Data (B and D) are means ± SEM

pooled from three independent experiments. *$P < 0.05$ and **$P < 0.01$ by Student's t test. Ub, ubiquitin.